24. WHAT CAUSED THE RECORD-BREAKING HEAT ACROSS AUSTRALIA IN OCTOBER 2015?

Pandora Hope, Guomin Wang, Eun-Pa Lim, Harry H. Hendon, and Julie M. Arblaster

Using a seasonal forecasting framework for attribution, we find that half of the record heat anomaly across Australia in October 2015 can be attributed to increasing CO_2, with much of the rest due to internal atmospheric variability.

The Event. In 2015, Australia experienced another exceptionally warm spring, making the spring seasons of 2013, 2014, and 2015 the three warmest from 105 years of record (Trewin 2013). In 2015, October was the most extreme month (Fig. 24.1a), with the largest monthly mean daily maximum temperature (AusTmax) anomaly (+3.44°C, relative to 1961–90; 33.54°C absolute) of any month, surpassing the September 2013 AusTmax record of +3.41°C. The monthly mean daily minimum temperature was also a record high for October (+2.34°C), and the fourth largest positive anomaly of any month. More than half of the continent (54.7%) recorded the highest-on-record October maximum temperatures, exceeding the previous record of 22.3% in 1988. The heat was particularly focused in the south (Fig. 24.1a), associated with a number of weather systems that encouraged surface northerlies from the continental interior during the month (Australian Bureau of Meteorology 2015). Temperatures in the north were relatively cool. At inland locations, temperatures were consistently above average, leading to record warm monthly averages, but no daily records being set.

Climate conditions during October 2015 and their relationship to Australian Tmax. The global climate of October 2015 was extraordinary in various aspects, with many large-scale climate features in a phase generally linked to unusually warm temperatures across Australia. These included a strong El Niño (www.bom.gov.au/climate/enso/archive/ensowrap_20151110.pdf), with Niño-3.4 at +2.2°C, Niño-3 at +2.3°C, and Niño-4 at +1.4°C above the 1961–90 average. Niño-4 was the warmest October value since records began in 1870 (HadISST used for sea surface temperature-based indices; Rayner et al. 2003; KNMI climate explorer: climexp.knmi.nl). The southern Indian Ocean (30°–120°E and 0°–60°S) was the warmest on record to date for any month, with an anomaly of +0.63°C compared to the 1961–90 average, and the Indian Ocean dipole (IOD) was strongly positive (dipole mode index: +0.76, relative to 1961–90; Saji et al. 1999). El Niño together with a positive IOD is typically associated with warm conditions over Australia during September to November (White et al. 2013), although the influence from El Niño becomes more important later in the year.

While seasonally varying oceanic conditions favored warm conditions across Australia, on the intraseasonal time scale many atmospheric features also favored warm conditions during October 2015 (see details on the climate state on the POAMA-2 pages at http://poama.bom.gov.au/). In spring, negative southern annular mode (SAM; Marshall 2003), phase 2 and 3 of the Madden–Julian oscillation (MJO; Wheeler and Hendon 2004) and blocking in the Tasman Sea are all associated with warm conditions across southern Australia (Marshall et al. 2013; Hendon et al. 2007). During October 2015, the subtropical ridge was intense, associated with blocking over the Tasman Sea as indicated by the subtropical ridge index (STRHI; Marshall et al. 2013), which was greater than two standard deviations above the mean in the first half of the month. The SAM varied through the month, but was negative during two periods of strong heat, in the first week and again around 20 October. From 23 October through the end of the month, the MJO became moderate to strong in Phase 2. The combination of these climatic features would be expected to bring heat to southern Australia.

AFFILIATIONS: Hope, Wang, Lim, and Hendon—Research and Development Branch, Bureau of Meteorology, Melbourne, Victoria, Australia; Arblaster—National Center for Atmospheric Research, Boulder, Colorado, and the School of Earth, Atmosphere and Environment, Monash University, Melbourne, Victoria, Australia

DOI:10.1175/BAMS-D-16-0142.1

A supplement to this article is available online (10.1175/BAMS-D-16-0142.2)

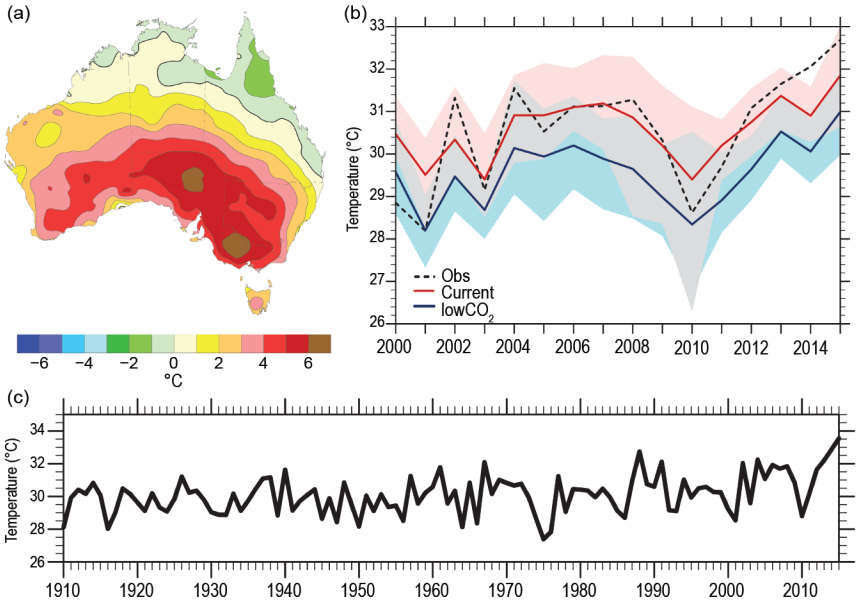

Fig. 24.1. (a) Map of observed anomaly of Oct 2015 mean Australian Tmax relative to 2000–14 climatology (Australian Water Availability Project; Jones et al. 2009). (b) The observed Oct AusTmax and ensemble mean Oct forecasts for current CO_2 conditions and 1960 (low CO_2) conditions. The ensemble range of 11 members forecast from 1 Oct each year is shown in pink shading for current CO_2 conditions and blue for low CO_2 conditions, and (c) time series of observed Oct AusTmax from 1910 to 2015.

Assessing the influence from increasing CO_2. Black and Karoly (2016) assessed the level of influence from anthropogenic climate change on the October 2015 heat across southern Australia. Probabilities of the current climate were estimated using very large ensembles of simulations (over 2000 realizations) from the HadRM3P nested regional atmospheric GCM forced with 2015 sea surface temperatures (SSTs). The natural world probabilities were from similar experiments where a measure of the impact of anthropogenic forcing since preindustrial times had been removed (weather@home; Black et al. 2015). They calculated the fraction of attributable risk (FAR; Stott et al. 2004) of exceeding the previous temperature record for southern Australia. Defining FAR = 1 – (P1 / P2), where P1 is the probability of exceeding the previous threshold in the "natural" world, and P2 is the probability of exceeding the previous threshold in the current world. They found a conservative FAR estimate of 0.76. A FAR of 0.76 means that October 2015 was at least four times more likely to exceed the previous record, set in 2014, of 29.68°C in the current world than in the natural world.

Here, extending the method of Hope et al. (2015), we use a fully coupled seasonal forecast modeling system to attribute the level of influence of both the last 55 years of increasing CO_2 and natural (internal) variability on this event. The Australian Bureau of Meteorology's seasonal forecast model POAMA-2.4 (Cottrill et al. 2013; Hudson et al. 2013) was used. Note that the use of a coupled seasonal forecast system in this way is unique and has certain limitations and strengths compared to other methods. For instance, the initial-value nature of the framework allows little time for the growth of model-driven biases, while allowing the full coupled response of the ocean–atmosphere–land system. Currently, only changes in CO_2 are considered and not other anthropogenic factors such as land-use change or aerosols. For full details of the method used here, refer to Wang et al. (2016).

For each of 24 September, 27 September, and 1 October 2015, an 11-member ensemble forecast of October 2015 under current CO_2 levels (400 ppm) was initialized with observed atmosphere, ocean, and land conditions, forming a 33-member ensemble. A corresponding ensemble forecast was also initialized on the same dates, but with CO_2 set to the 1960 level of 315 ppm and with anomalies—corresponding to the signature of change due to the last 55 years of rising CO_2—removed from the ocean, soil, and atmosphere to create a "low CO_2" forecast. For the three-dimensional ocean, the signature of change due to rising CO_2 levels was the difference between the ocean state in the final years of long integrations with fixed CO_2 at 400 or 315 ppm. To calculate the signature of change in the atmosphere or land, differences were made between two sets of forecasts for October 2015 using either current initial conditions or the current initial conditions with 315 ppm and the ocean state after subtracting the difference as calculated above. Two forecast climatologies, one for the current climate and one for the low CO_2 climate, were produced with an ensemble of 11 members initialized on 1 October for each year from 2000–14. Although short, this 15-year period includes a range of interannual variability due to the different states of ENSO. The climatology

has 165 members (11 forecasts for each October, 15 in total). The time series of the ensemble mean forecasts and the forecast spread of the two experiments are shown in Fig. 24.1b. The probability distribution functions (PDFs) are shown in Fig. 24.2b.

The record heat across Australia in October 2015 was well predicted under current CO_2 levels; the 2015 ensemble mean was warmer than any year in the 2000-14 climatology (Fig. 24.1b, red line). Although the ensemble mean anomaly was less than observed, one forecast ensemble member was warmer than observed (Fig. 24.2a). The forecast for October 2015 under the current climate was 2.0°C warmer than the low CO_2 climatology mean (Fig. 24.2a, red dot compared to blue line) The ensemble mean of the October 2015 forecast in the low CO_2 climate was the warmest ensemble mean against the low CO_2 climatology (Fig. 24.1b, blue line). Thus even under low CO_2 conditions, forecasts driven by the observed state of the internal atmospheric variability were the warmest on record.

An obvious measure of the contribution from increasing CO_2 is simply the difference between the two means of the current and low CO_2 forecast climatologies, which is 1.0°C and statistically significant ($p < 0.01$) (Fig. 24.2, dashed lines). This aligns with the observed change of 1.1°C from around 1960 (1953–67) to recent years (2000–14), see Fig. 24.1c.

To calculate an estimate of the FAR, the previous record was taken as the warmest ensemble mean forecast in the climatology under current CO_2 levels, with a value of 31.4°C. Across the 33-member forecast ensemble of 2015, five members exceeded this threshold in the low CO_2 climate, while 17 exceeded it in the current climate, leading to a FAR value of 0.71. Alternatively, if the previous record was taken from observations (32.1°C, set in 2014), none of the ensemble members of the 2015 forecast in a low CO_2 climate exceeded this threshold, while six ensemble members exceeded it in the current climate, thus the FAR would be 1.0.

Assessing the influence from the climatic and synoptic conditions. In order to further explore the importance of the atmospheric state (e.g., MJO, the location of the subtropical ridge, SAM) as compared to the antecedent land conditions or the oceanic state (e.g., El Niño, IOD) for promoting the record warmth, further forecast experiments were done, removing the influence from either the land, ocean, or atmosphere initial conditions, following Arblaster et al. (2014) and Wang et al. (2016). The results (outlined in more detail in the online supplemental material) indicate that the overwhelming driver of the heat was the atmospheric state from the atmospheric initial conditions, as opposed to the ocean or land state. This suggests that the direct impact on warming from the strong El Niño and IOD was small, and the major impact was from intraseasonal drivers such as MJO activity in the tropical Indian Ocean, the negative SAM, and Tasman Sea blocking.

Conclusions. Using a seasonal forecast framework, the record heat of October 2015 across Australia was attributed to the last 55 years of CO_2 induced warming and other factors. The warming from CO_2 contributed roughly 1.0°C to the extreme heat forecast across Australia in October 2015, while a combination of Tasman Sea blocking, negative SAM, MJO, and a high positioned over the southeast of the country, on

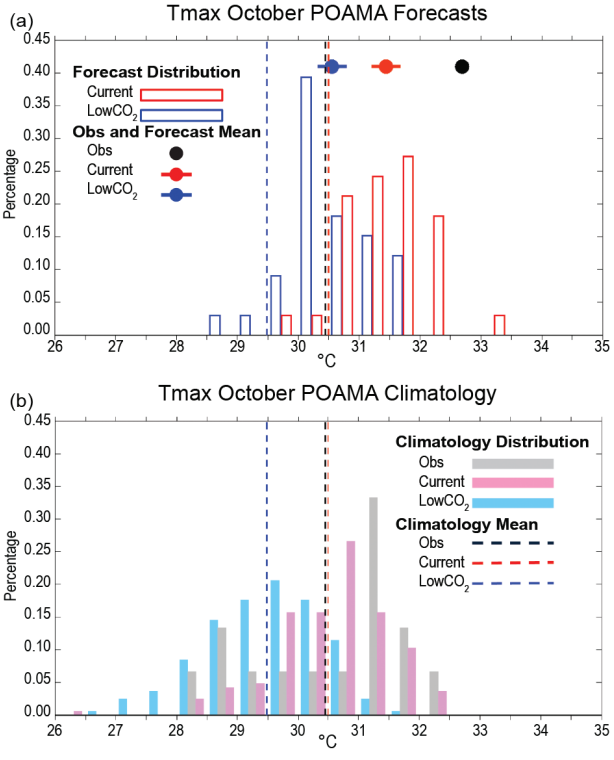

Fig. 24.2. (a) The distribution of the forecast Oct 2015 AusTmax is estimated with 33 member forecasts for current (red open bars) and low CO_2 (blue open bars) climates. The mean value for the observed event in Oct 2015 is shown by the top black dot, with the event ensemble means for current in red and low CO_2 in blue. (b) Oct AusTmax climatology distribution for 2000–14 from observations (gray bars), and the climatology estimated using 11 member Oct forecasts during 2000–14 for the current climate (pink solid bars) and the low CO_2 climate of 1960 (light blue solid bars). The climatology means are shown in dashed lines: black for observations, red for current, and blue for low CO_2.

the background state of a strong El Niño and a positive IOD, all contributed to the remaining 1.0°C of the 2.0°C forecast anomaly against a 1960, low CO_2 climatology. The FAR estimate for October 2015 Aus-Tmax being warmer than the previous record using this framework was 0.71, similar to the 0.76 that Black and Karoly (2016) showed for southern Australia. The pattern of anomalously low pressure to the south of Australia and a high over the southeast of the continent appears to be a consistent feature of the extreme heat across southern Australia during the last three springs of 2013 (Arblaster et al. 2014), 2014 (Hope et al. 2015; Gallant and Lewis 2016), and 2015.

ACKNOWLEDGEMENTS. Thank you to reviews from Robert Colman, Debra Hudson, and two anonymous reviewers who improved the manuscript. This project was in part supported through funding from the Australian Government's National Environmental Science Programme.

REFERENCES

Arblaster, J. M., E. Lim, H. H. Hendon, B. C. Trewin, M. C. Wheeler, G. Liu, and K. Braganza, 2014: Understanding Australia's hottest September on record [in "Explaining Extreme Events of 2013 from a Climate Perspective"]. *Bull. Amer. Meteor. Soc.*, **95 (9)**, S37–S41.

Australian Bureau of Meteorology, 2015: Special Climate Statement 52 (update): Australia's warmest October on record. Bureau of Meteorology, 21 pp. [Available online at www.bom.gov.au/climate/current/statements/scs52.pdf.]

Black, M. T., and D. J. Karoly, 2016: Southern Australia's warmest October on record: The role of ENSO and climate change [in "Explaining Extreme Events of 2015 from a Climate Perspective"]. *Bull. Amer. Meteor. Soc.*, **97 (12)**, S118–S121, doi10.1175/BAMS-D-16-0124.1. (chapter 20 of EEE)

——, ——, and A. D. King, 2015: The contribution of anthropogenic forcing to the Adelaide and Melbourne, Australia, heat waves of January 2014 ["in Explaining Extreme Events of 2014 from a Climate Perspective"]. *Bull. Amer. Meteor. Soc.*, **96 (12)**, S145–S148, doi:10.1175/BAMS-D-15-00097.1.

Cottrill, A., and Coauthors, 2013: Seasonal forecasting in the Pacific using the coupled model POAMA-2. *Wea. Forecasting*, **28**, 668–680, doi:10.1175/WAF-D-12-00072.1.

Gallant, A. J. E., and S. C. Lewis, 2016: Stochastic and anthropogenic influences on repeated record-breaking temperature extremes in Australian spring of 2013 and 2014. *Geophys. Res. Lett.*, **43**, 2182–2191, doi:10.1002/2016GL067740.

Hendon, H., D. W. J. Thompson, and M. C. Wheeler, 2007: Australian rainfall and surface temperature variations associated with the Southern Hemisphere annular mode. *J. Climate*, **20**, 2452–2467, doi:10.1175/JCLI4134.1.

Hope, P., E.-P. Lim, G. Wang, H. H. Hendon, and J. M. Arblaster, 2015: Contributors to the record high temperatures across Australia in late spring 2014 ["in Explaining Extremes. 2014 from a Climate Perspective"]. *Bull. Amer. Meteor. Soc.*, **96 (12)**, S149–S153, doi:10.1175/BMAS-D-15-00096.1.

Hudson, D., A. G. Marshall, Y. Yin, O. Alves, and H. H. Hendon, 2013: Improving intraseasonal prediction with a new ensemble generation strategy. *Mon. Wea. Rev.*, **141**, 4429–4449, doi:10.1175/MWR-D-13-00059.1.

Jones, D. A., W. Wang, and R. Fawcett, 2009: High-quality spatial climate data-sets for Australia. *Aust. Meteor. Oceanogr. J.*, **58**, 233–248.

Marshall, A., D. Hudson, M. Wheeler, O. Alves, H. Hendon, M. Pook, and J. Risbey, 2013: Intra-seasonal drivers of extreme heat over Australia in observations and POAMA-2. *Climate Dyn.*, **43**, 1915–1937, doi:10.1007/s00382-013-2016-1.

Marshall, G. J., 2003: Trends in the southern annular mode from observations and reanalyses. *J. Climate*, **16**, 4134–4143.

Rayner, N. A., D. E. Parker, E. B. Horton, C. K. Folland, L. V. Alexander, D. P. Rowell, E. C. Kent, and A. Kaplan, 2003: Global analyses of sea surface temperature, sea ice, and night marine air temperature since the late nineteenth century. *J. Geophys. Res.*, **108**, 4407, doi:10.1029/2002JD002670.

Saji, N., G. Goswami, P. Vinayachandran, and T. Yamagata, 1999: A dipole mode in the tropical Indian Ocean. *Nature*, **401**, 360–363.

Stott, P., D. Stone, and M. Allen, 2004: Human contribution to the European heatwave of 2003. *Nature*, **432**, 610–614.

Trewin, B., 2013: A daily homogenized temperature data set for Australia. *Int. J. Climatol.*, **33**, 1510–1529, doi:10.1002/joc.3530.

Wang, G., P. Hope, E.-P. Lim, H. H. Hendon, and J. M. Arblaster, 2016: Three methods for the attribution of extreme weather and climate events. Bureau of Meteorology Research Report 018, 32 pp. [Available online at www.bom.gov.au/research/research-reports.shtml]

Wheeler, M. C., and H. H. Hendon, 2004: An all-season real-time multivariate MJO index: Development of an index for monitoring and prediction. *Mon. Wea. Rev.*, **132**, 1917–1932.

White, C. J., D. Hudson, and O. Alves, 2013: ENSO, the IOD and the intraseasonal prediction of heat extremes across Australia using POAMA-2. *Climate Dyn.*, **43**, 1791–1810, doi:10.1007/s00382-013-2007-2.